

5-7-2014

Magnetism of Zn-Doped SnO₂: Role of Surfaces

Pushpa Raghani
Boise State University

Balaji Ramanujam

Magnetism of Zn-doped SnO₂: Role of surfaces

Raghani Pushpa^{a)} and Balaji Ramanujam

Department of Physics, Boise State University, 1910 University Dr., Boise, Idaho 83725, USA

(Presented 8 November 2013; received 23 September 2013; accepted 14 October 2013; published online 21 February 2014)

Surface effects on the magnetization of Zn-doped SnO₂ are investigated using first principles method. Magnetic behavior of Zn-doped bulk and highest and lowest energy surfaces—(001) and (110), respectively, are investigated in presence and absence of other intrinsic defects. The Zn-doped (110) and (001) surfaces of SnO₂ show appreciable increase in the magnetic moment (MM) compared to Zn-doped bulk SnO₂. Formation energies of Zn defects on both the surfaces are found to be lower than those in bulk SnO₂. Zn doping favors the formation of oxygen vacancies. The density of states analysis on the Zn-doped (110) surface reveals that the spin polarization of the host band occurs primarily from p-orbitals of bridging oxygen atoms and the Zn atom itself contributes minimally. The present work provides a key understanding on the role played by the surfaces in inducing the magnetism of doped nanoparticles and thin films. © 2014 AIP Publishing LLC. [<http://dx.doi.org/10.1063/1.4859995>]

The Diluted magnetic semiconductors (DMSs) are known for their potential applications in spintronic¹ and optoelectronic² devices. Nanoparticles of wide bandgap semiconductors such as SnO₂,³ TiO₂,⁴ and ZnO⁵ are shown to display magnetic behavior in presence of magnetic and nonmagnetic dopants. Among the metal oxide diluted magnetic semiconductor (MODMS), SnO₂ is very interesting because of its bandgap (~3.6 eV), high optical transparency, electrical conductivity, and chemical sensitivity.⁶ Hence, SnO₂ has gained attraction for applications in solar cells, heat mirrors, catalysis, and gas sensing applications. Recent experimental reports on transition metal (TM)-doped (V,⁷ Cr,⁸ Mn,⁹ Fe,¹⁰ Co,¹¹ Ni,¹² Cu,¹³ and Zn¹⁴) SnO₂ have shown promising application on the high temperature ferromagnetic semiconductors. Theoretical and computational studies on the TM-doped (Co,¹⁵ Mn,¹⁶ Ni,¹⁷ Cu,¹⁸ and Zn^{19,20}) SnO₂ have also been performed to understand the induced magnetism. Despite a large number of experimental and theoretical investigations, induced magnetism of doped SnO₂ is still not very well understood. Almost all the previous theoretical investigations have exclusively focused on the bulk magnetism of doped and undoped SnO₂. However, in nanoparticles and thin films, surface-to-volume ratio is significantly high. Recently, Zhang *et al.*²¹ studied the surface magnetism induced by Co-doped (110) surface of SnO₂; Bouamra *et al.*²² studied the magnetic properties of Rh-doped (110) surface of SnO₂, and Rahman and Garcia-Suarez²³ studied the surface magnetism induced by a C-doped (001) surface. However, till date, there have not been any reports on the magnetism induced by nonmagnetic and metallic atom doped SnO₂ surfaces.

In this paper, we have studied the role of (110) and (001) surfaces of SnO₂ on the induced magnetism of Zn-doped SnO₂ nanoparticles using density functional theory. We have studied the structure, electronic, and magnetic properties of Zn-doped bulk (001) and (110) surfaces of SnO₂ in the presence and

absence of intrinsic defects such as oxygen and tin vacancies to understand their influence on the energetics and magnetic behavior. Our results provide an insight on the importance of surfaces in inducing the magnetism in nonmagnetic and metallic atom doped SnO₂ nanoparticles and thin films.

To investigate the structural, electronic, and magnetic properties of various point defects in bulk SnO₂ and on its (001) and (110) surfaces, we have used density functional theory (DFT) in the pseudopotential formalism as implemented in Quantum-ESPRESSO.^{24,25} The generalized gradient approximation (GGA) is employed for the exchange-correlation potential with Perdew-Burke-Ernzerhof (PBE) functional. SnO₂ crystallizes in the rutile structure and we find the lattice parameters as: $a = b = 4.843 \text{ \AA}$ and $c = 3.314 \text{ \AA}$. These lattice parameters compare well with earlier GGA calculations²⁶ and from experimental values.²⁷ The $1 \times 1 \times 1$ unit cell of SnO₂ contains two Sn and four oxygen atoms a Monkhorst-Pack²⁸ k-mesh of $6 \times 6 \times 9$ is adopted. A plane wave kinetic energy cutoff of 100 Ry was used for all calculations and forces were converged to 0.01 eV/Å. Surfaces of SnO₂ were modeled using a 2×2 supercell of symmetric and asymmetric slabs. The symmetric slabs contained seven atomic layers and a vacuum of ~13 Å. Central 3-layers were fixed at their bulk-like sites, and rest of the layers on top and bottom of the slabs were allowed to relax. The asymmetric slabs contained five atomic layers, having bottom three layers fixed at bulk-like sites.

We find that the band gap of SnO₂ with GGA is 0.7 eV in good comparison with previous GGA values of 0.6 eV,²⁹ 0.95 eV³⁰ but the experimental value is 3.6 eV.³¹ It is known that GGA underestimates the band gap of oxide materials.³² The surface energies of (001) surface was found to be 1.82 J/m², this compares well with the previously calculated GGA values of 1.72 J/m².³³ The surface energy of (110) surface was found to be 0.98 J/m² and it compares well with 1.01 J/m².³⁴ Thus, we correctly predict that (001) surface is higher in energy than the (110) Formation of dominant surface would depend on the preparation conditions (annealing temperature) during synthesis.³⁵ We find that the enthalpy of formation for the SnO₂ from

^{a)}Author to whom correspondence should be addressed. Electronic mail: pushparaghani@boisestate.edu.

metallic Sn and molecular oxygen (O_2) is -4.39 eV, which compares well with the value -4.51 eV³⁶ obtained from a previous DFT-GGA calculations and the experimental value of -5.99 eV/SnO₂.³⁷ This slight difference is presumably due to the self-interaction error in solids with local density approximation/GGA^{38,39} as shown in the density of states for the rutile phase of bulk SnO₂. The undoped bulk SnO₂, symmetric and asymmetric slabs of (001) and (110) surfaces were found to be non-magnetic, which compares well with previous theoretical^{26,28,36} and experimental^{42,43} observations.

In agreement with previous theory^{26,40,41} and experiments,⁴⁴ neutral and doubly ionized oxygen vacancies are found to be nonmagnetic in bulk SnO₂. However, singly ionized oxygen vacancy is found to be magnetic with a total magnetization of $0.35 \mu_B$. Wang *et al.*⁴⁵ also showed that singly ionized oxygen vacancies induce magnetization in bulk SnO₂. Neutral and doubly ionized oxygen vacancies on (001) and (110) surfaces are also found to be non-magnetic as in the case of bulk; this is in agreement with previous DFT-GGA results.²³ However, singly ionized oxygen vacancies are found to be magnetic on (001) surface and nonmagnetic (110) surface.

Tin vacancies, however, are found to be magnetic in bulk in agreement with previous calculations.^{26,41} We find that Sn vacancies are also magnetic on both the (001) and (110) surfaces. Magnetic moment (MM) of Sn vacancies is the same on (110) and (001) surfaces. This suggests that the energy of the surface or its geometry do not have much influence on the MM of Sn vacancies. The MM of Sn vacancies on surfaces is found to be similar to that of Sn vacancies in nanosheets of SnO₂.⁴⁰

We find that the MM of Sn vacancy on the symmetric and asymmetric slabs on (001) and (110) is the same. However, its MM is zero on the symmetric (001) and nonzero on the asymmetric (001) surface. The vanishing magnetic moment of the tin vacancy on symmetric slab of (001) surface suggests that the easy axis of magnetization for the V_{Sn} is out of the plane, i.e., perpendicular to the (001) surface, which at the top and the bottom of the slab cancel each other. However, the easy axis of magnetisation is in the surface plane for V_{Sn} on (110) surface, hence the two symmetric defects add up their magnetic moment.

Here, we focus mainly on neutral Sn vacancies because they are the primary source of magnetism in SnO₂.^{26,40,41} and Zn is also found to be more stable at Sn-site than at O-site. Formation energies (FE) of neutral oxygen and Sn vacancies in bulk and on surfaces are shown in Table I. In general, we find that both Sn and oxygen vacancies are easier to create on surfaces than in bulk. Further, they are easier to form on (001) surface rather than on (110) surface. This can be attributed to the higher surface energy of (001) surface than (110) surface.

It is well known^{19,20} that doping SnO₂ with Zn induces magnetism in bulk. Doping oxide materials with transition metals—magnetic or nonmagnetic atoms, like Fe, Co, and Cu induces magnetic moment^{11,46} in the nanoparticles. It has also been found that even nonmagnetic-nonmetallic atoms like C, N, and nonmagnetic, alkali metallic atoms like Mg, K can also induce magnetism in oxides.^{23,47} Nanoparticles having radius of only a few nanometers will have a large surface-to-volume ratio. The effect of surfaces in inducing the magnetism in oxide nanoparticles while doped with either magnetic or nonmagnetic atoms has not been investigated in detail. In the present work,

TABLE I. Defect formation energies (in eV) of oxygen and Sn vacancies in bulk and on surfaces within Sn-rich and O-rich conditions.

System	Defects	Sn-rich	O-rich	M_{cell} ($\mu_B/cell$)
Bulk	V_O^0	1.08	3.27	0.00
	V_{sn}^0	11.47	7.08	3.98
S-(001)	V_O^0	-1.68	0.51	0.00
	V_{sn}^0	9.01	4.62	0.00
S-(110)	V_O^0	-0.64	1.56	0.00
	V_{sn}^0	10.10	5.71	4.00

we perform a consistent study of magnetism in doped bulk as well as surfaces of SnO₂ in order to understand the role of surfaces in inducing the magnetism with a nonmagnetic atom doping. Zn-doped SnO₂ is taken as the case study to understand the surface effects.

To understand the role of surfaces, Zn is incorporated at Sn-site in surface and subsurface layers of SnO₂. The total magnetization of Zn-doped (001) or (110) surface was found to increase by about $\sim 40\%$ compared to that of Zn-doped bulk alone. It is known that when Zn substitutes Sn-atom in bulk SnO₂, the nearest neighbor (NN) oxygens get their p-orbitals spin polarized due to the holes generated by Zn atom and thus contribute to the net magnetic moment. In the case of Zn-doped (001) surface, Zn is surrounded by four oxygens instead of six, therefore the same number of holes generated by Zn polarize fewer oxygens, which results into a larger magnetic moment. In the case of (110) surface, the Zn polarizes the bridging oxygen atoms to a larger extent than in-plane oxygens. Zn atom itself does not get polarized in all the cases. The subsurface Zn doping on (001) and (110) surfaces also showed similar magnetic moment per cell as that of surface doping. When the doping is done on the bulk-like sites of the (001) and (110) surfaces, the total magnetic moment of the (001) slab was found to be almost comparable to that of the (110) surface and the bulk calculation. All these results (Table II) show that the MM of Zn-doped SnO₂ is greatly affected by the presence of surfaces.

FEs of Zn defects on surfaces are calculated to gauge the feasibility of formation of Zn defects on surfaces. We find that the FE of Zn_{Sn} is half of the FE in bulk, whereas on (110) surface, FE is very similar to that in bulk. On (001) surface, FEs increase as Zn goes in the subsurface and

TABLE II. Defect formation energies (in eV) and magnetic moments (μ_B) of isolated Zn_{Sn} defects in bulk, on (001) and (110) surface. Zn_{Sn}^B , Zn_{Sn}^{11} , Zn_{Sn}^{12} , Zn_{Sn}^f indicate the position of Zn atom in bulk, surface layer, subsurface layer (2nd layer in slab), and in frozen part of the slab, respectively. M_{cell} and M_{Zn} are magnetic moments of the whole cell and Zn atom alone.

System	Defects	Sn-rich	O-rich	M_{cell} ($\mu_B/cell$)	M_{Zn} (μ_B/Zn)
Bulk	Zn_{Sn}^B	4.68	0.29	1.42	0.11
	Zn_{Sn}^{11}	2.80	-1.59	1.96	0.10
	Zn_{Sn}^{12}	3.65	-0.74	2.00	0.00
(001)	Zn_{Sn}^f	4.83	0.44	1.85	0.11
	Zn_{Sn}^{11}	4.02	-0.37	2.00	0.00
	Zn_{Sn}^{12}	4.30	-0.09	1.97	0.08
(110)	Zn_{Sn}^f	4.61	0.23	1.29	0.00

eventually in bulk. However, the FEs on (110) are almost constant while going from surface to subsurface to bulk. Again, the FE of Zn_{Sn} on (001) is lower than that of the (110) surface as found for oxygen and tin vacancies.

Spin resolved density of states studies are performed to understand the origin of magnetism in Zn-doped SnO_2 surfaces. Figures 1(a)–1(d) show the partial density of states (PDOS) of nearest neighbour bridging and in-plane oxygens, Sn and Zn atoms on the Zn-doped (110) surface, respectively. Unlike the Zn-doped bulk, the Zn atom on the (110) surface does not contribute to the induced magnetic moment. The PDOS of the NN bridging oxygen atom (Figure 1(c)) shows larger asymmetry on the p-orbital states in the conduction band minima as well as in the valence band maxima, which mainly contributes to the asymmetry on the TDOS of the Zn-doped (110) surface. The magnetic moment induced by the NN bridging oxygen was found to be $0.925 \mu_B$. The PDOS of the NN in-plane oxygen atom (Figure 1(d)) shows asymmetry on the states arising from their p-orbitals, but their contribution to the TDOS is very small, which is clearly shown in its contribution ($0.039 \mu_B$) to the total magnetic moment. The PDOS of the NN Sn atom shows an asymmetry in the states of conduction band minima, arising from the d-orbital, but the contribution of this asymmetry to the TDOS of the Zn-doped system is minimal, evident from the magnetic moment of $0.038 \mu_B$ contributed to the total magnetisation. Overall, it can be observed that the asymmetry in the TDOS of the Zn-doped (110) surface is mainly from the NN bridging oxygens and minimally from the NN in-plane oxygen and Sn atom.

In summary, magnetism and energetics of isolated intrinsic and extrinsic defects, in bulk, on (001) and (110) surfaces are investigated to understand the role of surfaces in inducing the magnetism in Zn-doped SnO_2 . We find that neutral and doubly ionized oxygen vacancies do not induce magnetism in bulk and on surfaces, while singly ionized oxygen vacancies do induce magnetism in bulk and on (001) surface only. The oxygen vacancies are much easier to create on surfaces than in bulk. Isolated neutral tin vacancies are found to produce a large MM, both in bulk and on surfaces; however, they are harder to create in bulk as well as on surfaces. Isolated Zn_{Sn} defects are

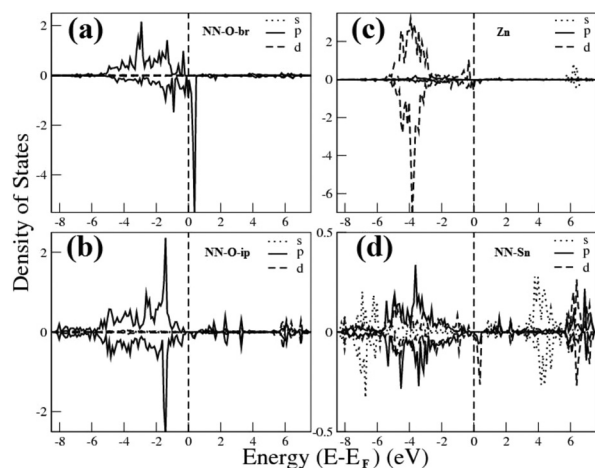


FIG. 1. Partial density of states of Zn-doped (110) surface: Near neighbor bridging oxygen (a), near neighbor in-plane oxygen (b), Zn (c), and near neighbor Sn (d).

found to have a larger magnetic moment on both the (001) and (110) surfaces than in bulk. Zn_{Sn} defects are much easier to create on (001) surface than in bulk but they are equally harder to create on (110) surfaces. These observations ascertain the role of surfaces in induced magnetism in Zn-doped SnO_2 .

We gratefully acknowledge the financial support from the Research Corporation Cottrell Scholar award and NSF CAREER award (DMR-1255584). Calculations were performed at the HPC Center of Idaho National Laboratory. We wish to thank Alex Punnoose and his group members from Boise State University for helpful discussions.

- ¹S. A. Wolf *et al.*, *Science* **294**(5546), 1488–1495 (2001).
- ²K. S. Burch, D. D. Awschalom, and D. N. Basov, *J. Magn. Magn. Mater.* **320**(23), 3207–3228 (2008).
- ³H. Jiang *et al.*, *Appl. Surf. Sci.* **258**(1), 236–241 (2011).
- ⁴B. Choudhury and A. Choudhury, *Curr. Appl. Phys.* **13**(6), 1025–1031 (2013).
- ⁵H. L. Liu *et al.*, *Phys. E-Low-Dimensional Systems & Nanostructures* **47**, 1–5 (2013).
- ⁶J. Hays *et al.*, *Phys. Rev. B* **72**(7), 075203 (2005).
- ⁷N. H. Hong and J. Sakai, *Phys. B: Condens. Matter* **358**(1–4), 265–268 (2005).
- ⁸N. H. Hong *et al.*, *J. Phys.: Condens. Matter* **17**(10), 1697–1702 (2005).
- ⁹C. B. Fitzgerald *et al.*, *Phys. Rev. B* **74**(11), 115307 (2006).
- ¹⁰J. M. D. Coey *et al.*, *Appl. Phys. Lett.* **84**(8), 1332–1334 (2004).
- ¹¹S. B. Ogale *et al.*, *Phys. Rev. Lett.* **91**(7), 077205 (2003).
- ¹²N. H. Hong *et al.*, *J. Phys.: Condens. Matter* **17**(41), 6533–6538 (2005).
- ¹³L. J. Li *et al.*, *J. Appl. Phys.* **107**(1), 014303 (2010).
- ¹⁴X. F. Liu *et al.*, *J. Phys. Chem. C* **114**(11), 4790–4796 (2010).
- ¹⁵H. X. Wang *et al.*, *J. Magn. Magn. Mater.* **321**(19), 3114–3119 (2009).
- ¹⁶Y. Lu *et al.*, *Phys. B-Condens. Matter* **406**(17), 3137–3141 (2011).
- ¹⁷H. X. Wang *et al.*, *J. Appl. Phys.* **107**(10), 103923 (2010).
- ¹⁸C. W. Zhang *et al.*, *Phys. Status Solidi B-Basic Solid State Physics* **246**(7), 1652–1655 (2009).
- ¹⁹Y. L. Zhang, X. M. Tao, and M. Q. Tan, *J. Magn. Magn. Mater.* **325**, 7–12 (2013).
- ²⁰L.-B. Shi *et al.*, *Mater. Sci. Semicond. Process.* **16**(3), 877–883 (2013).
- ²¹C. W. Zhang *et al.*, *Solid State Sci.* **13**(8), 1608–1611 (2011).
- ²²F. Bouamra *et al.*, *Appl. Surf. Sci.* **269**, 41–44 (2013).
- ²³G. Rahman and V. M. Garcia-Suarez, *Appl. Phys. Lett.* **96**(5), 052508 (2010).
- ²⁴P. Giannozzi *et al.*, *J. Phys.: Condens. Matter* **21**(39), 19 (2009).
- ²⁵N. Troullier and J. L. Martins, *Phys. Rev. B* **43**(3), 1993–2006 (1991).
- ²⁶G. Rahman *et al.*, *Phys. Rev. B* **78**(18), 184404 (2008).
- ²⁷J. Haines and J. M. Léger, *Phys. Rev. B* **55**(17), 11144–11154 (1997).
- ²⁸H. J. Monkhorst and J. D. Pack, *Phys. Rev. B* **13**(12), 5188–5192 (1976).
- ²⁹K. G. Godinho, A. Walsh, and G. W. Watson, *J. Phys. Chem. C* **113**(1), 439–448 (2009).
- ³⁰A. K. Singh *et al.*, *Phys. Rev. Lett.* **101**(5), 055502 (2008).
- ³¹A. L. Dawar and J. C. Joshi, *J. Mater. Sci.* **19**(1), 1–23 (1984).
- ³²Y. Z. Zhu *et al.*, *Phys. Rev. B* **77**(24), 245209 (2008).
- ³³J. Oviedo and M. J. Gillan, *Surf. Sci.* **463**(2), 93–101 (2000).
- ³⁴W. Bergermayer and I. Tanaka, *Appl. Phys. Lett.* **84**(6), 909–911 (2004).
- ³⁵M. Batzill and U. Diebold, *Progress Surf. Sci.* **79**(2–4), 47–154 (2005).
- ³⁶G. Novell-Leruth, G. Carchini, and N. Lopez, *J. Chem. Phys.* **138**(19), 194706 (2013).
- ³⁷“Tin dioxide (SnO_2) entropy, heat of formation,” in *Non-Tetrahedrally Bonded Elements and Binary Compounds I*, edited by O. Madelung, U. Rössler, and M. Schulz (Springer Berlin Heidelberg, 1998), pp. 1–2.
- ³⁸C. G. Van de Walle and A. Janotti, *Phys. Status Solidi B-Basic Solid State Physics* **248**(1), 19–27 (2011).
- ³⁹A. Janotti and C. G. Van de Walle, *Appl. Phys. Lett.* **87**(12), 122102 (2005).
- ⁴⁰G. Rahman, V. M. Garcia-Suarez, and J. M. Morbec, *J. Magn. Magn. Mater.* **328**, 104–108 (2013).
- ⁴¹G. Rahman *et al.*, *Phys. Rev. B* **87**(20), 205205 (2013).
- ⁴²G. S. Chang *et al.*, *Phys. Rev. B* **85**(16), 165319 (2012).
- ⁴³N. H. Hong, N. Poirrot, and J. Sakai, *Phys. Rev. B* **77**(3), 033205 (2008).
- ⁴⁴A. Espinosa *et al.*, *J. Phys. Chem. C* **115**(49), 24054–24060 (2011).
- ⁴⁵H. X. Wang *et al.*, *Phys. Status Solidi B* **247**(2), 444–448 (2010).
- ⁴⁶K. Ueda, H. Tabata, and T. Kawai, *Appl. Phys. Lett.* **79**(7), 988–990 (2001).
- ⁴⁷S. K. Srivastava *et al.*, *Phys. Rev. B* **82**(19), 193203 (2010).